# Upconversion luminescence from aluminoborate glasses doped with $Tb^{3+}$, $Eu^{3+}$ and $Dy^{3+}$ under the excitation of 2.6-μm femtosecond laser pulses

**M. H. Yuan,[1] H. H. Fan,[1] Q. F. Dai,[1] S. Lan,[1,*] X. Wan,[2] and S. L. Tie[2]**

[1]*Guangdong Provincial Key Laboratory of Nanophotonic Functional Materials and Devices, School of Information and Optoelectronic Science and Engineering, South China Normal University, Guangzhou, China*
[2]*School of Chemistry and Environment, South China Normal University, Guangzhou, China*
[*]*slan@scnu.edu.cn*

**Abstract:** We investigated the upconversion luminescence of three aluminoborate glasses doped with $Tb^{3+}$, $Eu^{3+}$, and $Dy^{3+}$ under the excitation of 2.6-μm femtosecond (fs) laser pulses. Efficient upconversion luminescence appearing in the visible light spectral region was observed in all three glasses and the emission spectra are quite similar to those obtained under single photon excitation. From the dependence of the luminescence intensity on the excitation intensity in the low excitation intensity regime, it was revealed that a four-photon process is involved in the generation of the upconversion luminescence in the $Tb^{3+}$- and $Eu^{3+}$-doped glasses while a mixed two- and three-photon process is involved in the $Dy^{3+}$-doped glass. In the high excitation intensity regime, a reduction of the slope to about 1.0 was observed for all glasses. A physical mechanism based on the super saturation of the intermediate states of the rare-earth ions was employed to interpret the upconversion luminescence under the excitation of long-wavelength fs laser pulses. Significantly broadened luminescence spectra were observed in thick glasses under high excitation intensities and it can be attributed to the self-focusing of the laser beam in the thick glasses.

©2015 Optical Society of America

**OCIS codes:** (160.5690) Rare-earth-doped materials; (190.4180) Multiphoton processes; (190.7220) Upconversion; (160.2750) Glass and other amorphous materials.

## References and links

1. G. Blasse and B. C. Grabmaier, *Luminescent Materials* (Springer-Verlag, 1994).
2. D. L. Huber, M. M. Broer, and B. Golding, "Low-temperature optical dephasing of rare-earth ions in glass," Phys. Rev. Lett. **52**(25), 2281–2284 (1984).
3. S. Zhang, B. Zhu, S. Zhou, S. Xu, and J. Qiu, "Multi-photon absorption upconversion luminescence of a $Tb^{3+}$-doped glass excited by an infrared femtosecond laser," Opt. Express **15**(11), 6883–6888 (2007).
4. A. B. Seddon, Z. Tang, D. Furniss, S. Sujecki, and T. M. Benson, "Progress in rare-earth-doped mid-infrared fiber lasers," Opt. Express **18**(25), 26704–26719 (2010).
5. D. L. Yang, H. Gong, E. Y. B. Pun, X. Zhao, and H. Lin, "Rare-earth ions doped heavy metal germanium tellurite glasses for fiber lighting in minimally invasive surgery," Opt. Express **18**(18), 18997–19008 (2010).
6. Ł. Sójka, Z. Tang, H. Zhu, E. Bereś-Pawlik, D. Furniss, A. B. Seddon, T. M. Benson, and S. Sujecki, "Study of mid-infrared laser action in chalcogenide rare earth doped glass with $Dy^{3+}$, $Pr^{3+}$ and $Tb^{3+}$," Opt. Mater. Express **2**(11), 1632–1640 (2012).
7. X. Han, E. Castellano-Hernández, J. Hernández-Rueda, J. Solís, and C. Zaldo, "White and full color upconversion film-on-glass displays driven by a single 978 nm laser," Opt. Express **22**(20), 24111–24116 (2014).
8. G. Zanella, R. Zannoni, R. DallIgna, B. Locardi, P. Polato, M. Bettinelli, and A. Marigo, "A new cerium cintillating glass for X-ray detection," Nucl. Instrum. Methods Phys. Res. A **345**(1), 198–201 (1994).
9. S. Huang and M. Gu, "Enhanced luminescent properties of $Tb^{3+}$ ions in transparent glass ceramics containing $BaGdF_5$ nanocrystalsm," J. Non-Cryst. Solids **358**(1), 77–80 (2012).
10. M. Nikl, "Scintillation detectors for x-rays," Meas. Sci. Technol. **17**(4), R37–R54 (2006).
11. S. Heer, K. Kömpe, H. U. Güdel, and M. Haase, "High efficient multicolour upconversion emission in transparent colloids of lanthanide-doped $NaYF_4$ nanocrystals," Adv. Mater. **16**, 2102–2105 (2004).

#243906 Received 29 Jun 2015; revised 7 Aug 2015; accepted 9 Aug 2015; published 12 Aug 2015
© 2015 OSA

12. R. T. Wegh, H. Donker, K. D. Oskam, and A. Meijerink, "Visible quantum cutting in $LiGdF_4:Eu^{3+}$ through downconversion," Science **283**(5402), 663–666 (1999).
13. D. Timmerman, I. Izeddin, P. Stallinga, I. N. Yassievich, and T. Gregorkiewicz, "Space-separated quantum cutting with silicon nanocrystals for photovoltaic applications," Nat. Photonics **2**(2), 105–109 (2008).
14. B. M. van der Ende, L. Aarts, and A. Meijerink, "Near-infrared quantum cutting for photovoltaics," Adv. Mater. **21**(30), 3073–3077 (2009).
15. B. M. van der Ende, L. Aarts, and A. Meijerink, "Lanthanide ions as spectral converters for solar cells," Phys. Chem. Chem. Phys. **11**(47), 11081–11095 (2009).
16. D. Serrano, A. Braud, J. L. Doualan, P. Camy, A. Benayad, V. Mnard, and R. Moncorg, "Ytterbium sensitization in $KY_3F_{10}$: $Pr^{3+}$, $Yb^{3+}$ for silicon solar cells efficiency enhancement," Opt. Mater. **33**(7), 1028–1031 (2011).
17. J. M. Meijer, L. Aarts, B. M. van der Ende, T. J. H. Vlugt, and A. Meijerink, "Downconversion for solar cells in $YF_3:Nd^{3+}$, $Yb^{3+}$," Phys. Rev. B **81**(3), 035107 (2010).
18. L. Aarts, B. M. van der Ende, and A. Meijerink, "Downconversion for solar cells in $NaYF_4$:Er,Yb," J. Appl. Phys. **106**(2), 023522 (2009).
19. B. S. Richards, "Luminescent layers for enhanced silicon solar cell performance: down-conversion," Sol. Energy Mater. Sol. Cells **90**(9), 1189–1207 (2006).
20. Y. Xu, X. Zhang, S. Dai, B. Fan, H. Ma, J. L. Adam, J. Ren, and G. Chen, "Efficient near-infrared down-conversion in $Pr^{3+}$-$Yb^{3+}$ codoped glasses and glass ceramics containing $LaF_3$ nanocrystals," J. Phys. Chem. C **115**(26), 13056–13062 (2011).
21. Q. Y. Zhang, G. F. Yang, and Z. H. Jiang, "Cooperative downconversion in $GdAl_3(BO_3)_4:RE^{3+},Yb^{3+}$ (RE=Pr, Tb, and Tm)," Appl. Phys. Lett. **91**(5), 051903 (2007).
22. E. Downing, L. Hesselink, J. Ralston, and R. Macfarlane, "A three-color, solid-state, three-dimensional display," Science **273**(5279), 1185–1189 (1996).
23. M. J. Weber, "Radiative and multiphonon relaxation of rare-earth ions in $Y_2O_3$," Phys. Rev. **171**(2), 283–291 (1968).
24. M. Nyk, R. Kumar, T. Y. Ohulchanskyy, E. J. Bergey, and P. N. Prasad, "High contrast in vitro and in vivo photoluminescence bioimaging using near infrared to near infrared up-conversion in $Tm^{3+}$ and $Yb^{3+}$ doped fluoride nanophosphors," Nano Lett. **8**(11), 3834–3838 (2008).
25. G. A. Sotiriou, D. Franco, D. Poulikakos, and A. Ferrari, "Optically stable biocompatible flame-made $SiO_2$-coated $Y_2O_3:Tb^{3+}$ nanophosphors for cell imaging," ACS Nano **6**(5), 3888–3897 (2012).
26. J. Liu, R. Wu, N. Li, X. Zhang, Q. Zhan, and S. He, "Deep, high contrast microscopic cell imaging using three-photon luminescence of β-($NaYF_4:Er^{3+}/NaYF_4$) nanoprobe excited by 1480-nm CW laser of only 1.5-mW," Biomed. Opt. Express **6**(5), 1857–1866 (2015).
27. J. F. Suyver, A. Aebischer, S. García-Revilla, P. Gerner, and H. U. Güdel, "Anomalous power dependence of sensitized upconversion luminescence," Phys. Rev. B **71**(12), 125123 (2005).
28. M. Pollnau, D. R. Gamelin, S. R. Lüthi, H. U. Güdel, and M. P. Hehlen, "Power dependence of upconversion luminescence in lanthanide and transition-metal-ion systems," Phys. Rev. B **61**(5), 3337–3346 (2000).
29. G. Chen, H. Liang, H. Liu, G. Somesfalean, and Z. Zhang, "Near vacuum ultraviolet luminescence of $Gd^{3+}$ and $Er^{3+}$ ions generated by super saturation upconversion processes," Opt. Express **17**(19), 16366–16371 (2009).
30. L. Yang, H. Song, L. Yu, Z. Liu, and S. Lu, "Unusual power-dependent and time-dependent upconversion luminescence in nanocrystals $Y_2O_3$: $Ho^{3+}/Yb^{3+}$," J. Lumin. **116**(1-2), 101–106 (2006).
31. V. Kumar, P. Rani, D. Singh, and S. Chawla, "Efficient multiphoton upconversion and synthesis route dependent emission tunability in $GdPO_4:Ho^{3+}$, $Yb^{3+}$ nanocrystals," RSC Advances **4**, 36101–36105 (2014).
32. J. Zhou, G. Chen, Y. Zhu, L. Huo, W. Mao, D. Zou, X. Sun, E. Wu, H. Zeng, J. Zhang, L. Zhang, J. Qiu, and S. Xu, "Intense multiphoton upconversion of $Yb^{3+}$-$Tm^{3+}$ doped β-$NaYF_4$ individual nanocrystals by saturation excitation," J. Mater. Chem. C Mater. Opt. Electron. Devices **3**(2), 364–369 (2015).
33. G. Chen, T. Y. Ohulchanskyy, A. Kachynski, H. Ågren, and P. N. Prasad, "Intense visible and near-infrared upconversion photoluminescence in colloidal $LiYF_4:Er^{3+}$ nanocrystals under excitation at 1490 nm," ACS Nano **5**(6), 4981–4986 (2011).
34. C. Joshi, K. Kumar, and S. B. Rai, "Upconversion and anomalous power dependence in $Ca_{12}Al_{14}O_{33}:Er^{3+}$ /$Yb^{3+}$ single phase nanophosphor," J. Appl. Phys. **105**(12), 123103 (2009).
35. D. R. Larson, W. R. Zipfel, R. M. Williams, S. W. Clark, M. P. Bruchez, F. W. Wise, and W. W. Webb, "Water-soluble quantum dots for multiphoton fluorescence imaging in vivo," Science **300**(5624), 1434–1436 (2003).
36. Y. D. Glinka, S. H. Lin, and Y. T. Chen, "Two-photon-excited luminescence and defect formation in $SiO_2$ nanoparticles induced by 6.4-eV ArF laser light," Phys. Rev. B **62**(7), 4733–4743 (2000).
37. X. Wang, J. Qiu, J. Song, J. Xu, Y. Liao, H. Sun, Y. Cheng, and Z. Xu, "Upconversion luminescence and optical power limiting effect based on two- and three-photon absorption processes of ZnO crystal," Opt. Commun. **280**(1), 197–201 (2007).
38. K. Berland and G. Shen, "Excitation saturation in two-photon fluorescence correlation spectroscopy," Appl. Opt. **42**(27), 5566–5576 (2003).
39. K. Dunphy and W. W. Dule, "Multiphoton excitation of the 520 nm luminescence band in MgO:Al," Phys. Status Solidi **148**(2), 729–735 (1988).
40. J. Dai, M. H. Yuan, J. H. Zeng, Q. F. Dai, S. Lan, C. Xiao, and S. L. Tie, "Controllable color display induced by excitation-intensity-dependent competition between second and third harmonic generation in ZnO nanorods," Appl. Opt. **53**(2), 189–194 (2014).

#243906 Received 29 Jun 2015; revised 7 Aug 2015; accepted 9 Aug 2015; published 12 Aug 2015
© 2015 OSA

41. M. H. Yuan, H. Li, J. H. Zeng, H. H. Fan, Q. F. Dai, S. Lan, and S. T. Li, "Efficient blue light emission from $In_{0.16}Ga_{0.84}N$/GaN multiple quantum wells excited by 2.48-μm femtosecond laser pulses," Opt. Lett. **39**(12), 3555–3558 (2014).
42. M. Durand, A. Jarnac, A. Houard, Y. Liu, S. Grabielle, N. Forget, A. Durécu, A. Couairon, and A. Mysyrowicz, "Self-guided propagation of ultrashort laser pulses in the anomalous dispersion region of transparent solids: a new regime of filamentation," Phys. Rev. Lett. **110**(11), 115003 (2013).
43. Y. Liu, Y. Brelet, Z. He, L. Yu, S. Mitryukovskiy, A. Houard, B. Forestier, A. Couairon, and A. Mysyrowicz, "Ciliary white light: optical aspect of ultrashort laser ablation on transparent dielectrics," Phys. Rev. Lett. **110**(9), 097601 (2013).
44. F. Silva, D. R. Austin, A. Thai, M. Baudisch, M. Hemmer, D. Faccio, A. Couairon, and J. Biegert, "Multi-octave supercontinuum generation from mid-infrared filamentation in a bulk crystal," Nat. Commun. **3**, 807 (2012).
45. M. Durand, K. Lim, V. Jukna, E. McKee, M. Baudelet, A. Houard, M. Richardson, A. Mysyrowicz, and A. Couairon, "Blueshifted continuum peaks from filamentation in the anomalous dispersion regime," Phys. Rev. A **87**(4), 043820 (2013).
46. G. Chen, H. Qiu, P. N. Prasad, and X. Chen, "Upconversion nanoparticles: design, nanochemistry, and applications in theranostics," Chem. Rev. **114**(10), 5161–5214 (2014).

## 1. Introduction

Rare-earth-ion-doped glasses have attracted great interest in recent years because of their numerous applications in making optical fibers, waveguide lasers, optical amplifiers, multicolor displayers, solid state lasers, mid-infrared lasers, and Q-switched devices etc [1–11]. Under the excitation of high-energy radiation such as ultraviolet or X ray, rare-earth-ion-doped glasses can emit strong luminescence covering the spectral region from violet to near infrared. In particular, the phenomenon of quantum cutting in which a photon of high energy is absorbed and converted to two or more photons with lower energies, has been demonstrated in rare-earth-ion-doped glasses [12]. This phenomenon has drawn great attention in the research and development of high-efficiency solar cells because it can significantly improve the conversion efficiency of photon to electricity and reduce heat generation [13–20]. Owing to their unique ladder-like energy states, rare-earth ions, especially the lanthanide ions, are considered as promising candidates not only for photon downconversion but also for photon upconversion [17–21]. For example, solid state full color display has been demonstrated by exploiting the photon upconversion in three lanthanide ions of $Pr^{3+}$, $Er^{3+}$, and $Tm^{3+}$ [22].

Recently, the upconversion luminescence of rare-earth-ion-doped glasses has received intensive studies due to their potential application in bioimaging where near infrared lasers are preferred in order to avoid the damage of biological tissues. In fact, these glasses are promising candidates for the generation of short wavelength radiation through multiphoton-induced absorption (MPA) because they possess numerous energy levels in the infrared, visible and violet regions [20–22]. In addition, the excited states of rare-earth ions generally have long lifetimes [23], which also support stepwise excitation in MPA. The efficient upconversion in combination with the long lifetimes of rare-earth ions make them attractive for imaging life cells. As compared with semiconductor colloidal quantum dots which are commonly used in bioimaging, rare-earth-ion-doped nanophosphors are independent of particle size and their emission can be tuned by doping with different lanthanide ions. In addition, they have good thermal stability and do not suffer from blinking and photobleaching. Therefore, they have been successfully employed in the imaging of cells [24–26].

Actually, rare-earth-ion-doped glasses are suitable materials for studying photon upconversion because of the abundant energy levels with long lifetimes and the good thermal stability. These energy levels act as intermediate states for sequential transitions in the MPA-induced upconversion. At high excitation intensities, these intermediate states are effectively populated, leading to the phenomenon of super saturation [27,28]. As a result, the number of simultaneously absorbed photons necessary for the upconversion is reduced and so is the excitation intensity required for upconversion [29–34]. In addition, these glasses are easy to be shaped and possess high transparency, low production cost, and good thermal stability. These properties make them more attractive as compared with other materials used for photon

#243906 Received 29 Jun 2015; revised 7 Aug 2015; accepted 9 Aug 2015; published 12 Aug 2015
© 2015 OSA

upconversion. So far, the longest excitation wavelength used for generating the upconversion luminescence in rare-earth-ion-doped glasses is about 1.5 μm [33]. It is interesting to know whether efficient upconversion luminescence can be generated by using fs laser pulses with much longer wavelengths.

In this article, three aluminoborate glasses doped with $Tb^{3+}$, $Eu^{3+}$, and $Dy^{3+}$ were synthesized and their upconversion luminescence generated by using 2.6-μm fs laser pulses was investigated. Efficient upconversion luminescence appearing in the visible light spectral region was observed in all three glasses and the emission spectra were quite similar to those obtained under single-photon excitation. From the dependence of the luminescence intensity on the excitation intensity in the low excitation intensity regime, it was revealed that a four-photon process is involved in the generation of the upconversion luminescence in the $Tb^{3+}$- and $Eu^{3+}$-doped glasses while a mixed two- and three-photon process is involved in the $Dy^{3+}$-doped glass. A physical mechanism based on the super saturation of the intermediate states of the ions was employed to interpret the upconversion luminescence under the excitation of long-wavelength fs laser pulses. Significantly broadened luminescence spectra were observed in thick glasses under high excitation intensities and it can be attributed to the self-focusing of the laser beam in the thick glasses.

## 2. Experimental details

The composition of the glass samples were CaO-$Al_2O_3$-$B_2O_3$-$RE_2O_3$ ($Ca_{1-x}AlB$: $RE^{3+}{}_x$, RE = 1Tb, Eu and Dy) (Tb: x = 0.3, Eu: x = 0.4 and Dy: x = 0.07). The glass samples were prepared using analytical reagents including $CaCO_3$, $Al(OH)_3$, $H_3BO_3$ and high-purity grade oxide $Tb_4O_7$ (99.99%), $Eu_2O_3$ (99.99%) and $Dy_2O_3$ (99.95%). The mixed batches were sintered at certain temperature and then melted at 1200°C for 3 hours in air. The melts were poured into a preheated stainless steel mold and cooled to room temperature in air. The resultant glasses were annealed at 500°C for 3 hours to release the inner stress. In all glass samples, the rare-earth ions replace $Ca^{2+}$ ions in the glass CaAlB for equal quality on molarity. Then the glasses were sliced and polished as 500-μm-thick sheets for optical measurements. The linear absorption spectra were measured by using an UV–Vis–NIR spectrometer (UV-3101PC, Shimadzu) and the emission and excitation spectra under single-photon excitation were measured by using a spectrometer (F-4600, Hitachi).

For the characterization of their upconversion luminescence induced by MPA, the fs laser light with a repetition rate of 1 kHz and a pulse duration of ~100 fs delivered by an optical parametric amplifier (OperA Solo, Coherent) was used to excite the sample at an angle of ~45°. The excitation wavelength ($\lambda_{ex}$) was chosen to be 2.6-μm which is the longest excitation wavelength available in our laboratory. A focusing lens with f = 150 mm was used to focus the fs laser light and the diameter of the excitation spot was estimated to be ~300 μm. The emitted light was collected by using another lens in the direction normal to the sample surface and directed to a spectrometer (7ISW3052, SOFN Instruments) for analysis. For the measurement of the excitation intensity dependence of the luminescence intensity, a beam split was inserted in the optical path to calibrate the pump power. A filter was used in front of the spectrometer to eliminate the scattered light of the excitation laser.

## 3. Results and discussion

### *3.1 Downconversion luminescence under single photon excitation*

The emission (red curves) and excitation (black curves) spectra of the three samples are shown in Fig. 1. The excitation wavelengths ($\lambda_{ex}$) for the emission spectra and the monitoring wavelengths ($\lambda_{em}$) for the excitation spectra are also provided. For the $Tb^{3+}$-doped glass shown in Fig. 1(a), the peaks observed in the excitation spectrum are assigned to the transitions of $^7F_6 \rightarrow {}^5K_8$ (247 nm), $^7F_6 \rightarrow ({}^5H_7, {}^5D_{0,1})$ (317 nm), $^7F_6 \rightarrow ({}^5L_9, {}^5G_4)$ (352 nm), $^7F_6 \rightarrow {}^5L_{10}$ (369 nm) $^7F_6 \rightarrow ({}^5D_3, {}^5G_6)$ (377 nm), and $^7F_6 \rightarrow {}^5D_4$ (485 nm), respectively. The emission spectrum

#243906 Received 29 Jun 2015; revised 7 Aug 2015; accepted 9 Aug 2015; published 12 Aug 2015
© 2015 OSA

exhibits four emission bands centered at 488, 544, 585 and 622 nm, corresponding to the transitions of $^5D_4 \rightarrow {}^7F_6$, $^5D_4 \rightarrow {}^7F_5$, $^5D_4 \rightarrow {}^7F_4$ and $^5D_4 \rightarrow {}^7F_3$, respectively. In Fig. 1(b), the two peaks appearing in the excitation spectrum of the $Eu^{3+}$-doped glass correspond to the transitions of $^7F_0 \rightarrow {}^5D_2$ (465 nm) and $^7F_0 \rightarrow {}^5D_1$ (533 nm). In the emission spectrum, the three emission bands centered at 577, 591, and 615 nm are attributed to the transitions of $^5D_0 \rightarrow {}^7F_0$, $^5D_0 \rightarrow {}^7F_1$, and $^5D_0 \rightarrow {}^7F_2$, respectively. For the $Dy^{3+}$-doped glass shown in Fig. 1(c), the seven peaks observed in the excitation spectrum represent the transitions of $^6H_{15/2} \rightarrow {}^4D_{7/2}$ (325 nm), $^6H_{15/2} \rightarrow {}^6P_{7/2}$ (351 nm), $^6H_{15/2} \rightarrow {}^6P_{5/2}$ (365 nm), $^6H_{15/2} \rightarrow {}^4M_{21/2}$ (388 nm), $^6H_{15/2} \rightarrow {}^4G_{11/2}$ (426 nm), $^6H_{15/2} \rightarrow {}^4I_{15/2}$ (453 nm), and $^6H_{15/2} \rightarrow {}^4F_{9/2}$ (473 nm), respectively. The two emission bands centered at 483 and 575 nm in the emission spectrum originate from the transitions of $^4F_{9/2} \rightarrow {}^6H_{15/2}$ and $^4F_{9/2} \rightarrow {}^6H_{13/2}$, respectively. Based on the theory of colorimetry, we can easily deduce the chromaticity coordinates for the three glasses from their emission spectra, as shown in Fig. 1(d). It can be seen that the luminescence colors of the $Tb^{3+}$-, $Eu^{3+}$- and $Dy^{3+}$-doped glasses appear to be green, red, and yellow, implying their potential applications in color display and bioimaging.

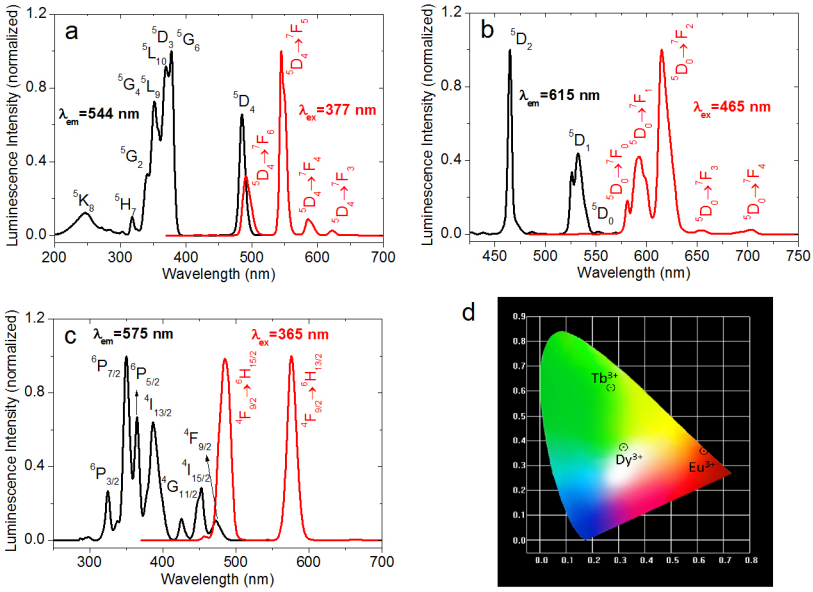


Fig. 1. Excitation (black curves) and emission (red curves) spectra for the aluminoborate glasses doped with $Tb^{3+}$ (a), $Eu^{3+}$ (b), and $Dy^{3+}$ (c) under single-photon excitation. $\lambda_{ex}$ and $\lambda_{em}$ are the excitation wavelengths for the emission spectra and the monitoring wavelengths for the excitation spectra. The CIE chromaticity coordinates calculated for the luminescence of the glasses are shown in (d).

### *3.2 Upconversion luminescence under multiphoton excitation in thin glass samples*

Having known the downconversion luminescence of the three glasses under single photon excitation, we wanted to study their upconversion luminescence induced via MPA by using fs laser pulses at 2.6 μm. We first examined the absorption of the three glasses in the near infrared spectral region, as shown Fig. 2. Appreciable absorption in the wavelength region of 1600-3000 nm was observed for all samples, implying the existence of many transitions in the rare-earth ions with transition energies in this wavelength region. The final energy states involved in the electronic transitions responsible for the absorption peaks are indicated in the corresponding absorption spectra. It is noticed that for all three samples the absorption at 2.6

#243906 Received 29 Jun 2015; revised 7 Aug 2015; accepted 9 Aug 2015; published 12 Aug 2015
© 2015 OSA

μm is appreciable. However, the largest absorption appears at ~2.8 μm, implying more efficient upconversion luminescence may be generated at this wavelength.

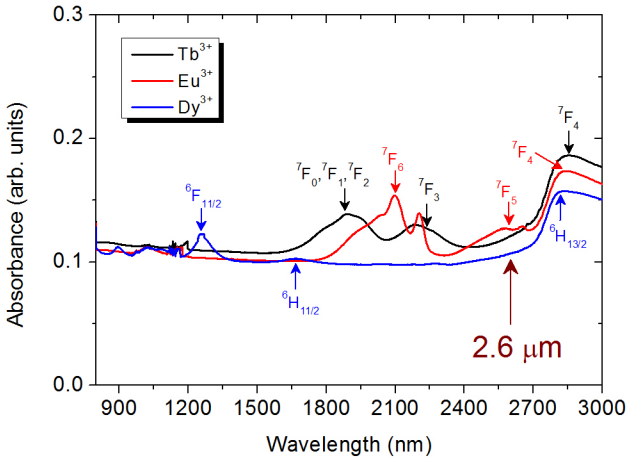


Fig. 2. Absorption spectra of the aluminoborate glasses doped with $Tb^{3+}$, $Eu^{3+}$, and $Dy^{3+}$ in the near infrared spectral region. The final states involved in the electronic transitions are indicated by arrows.

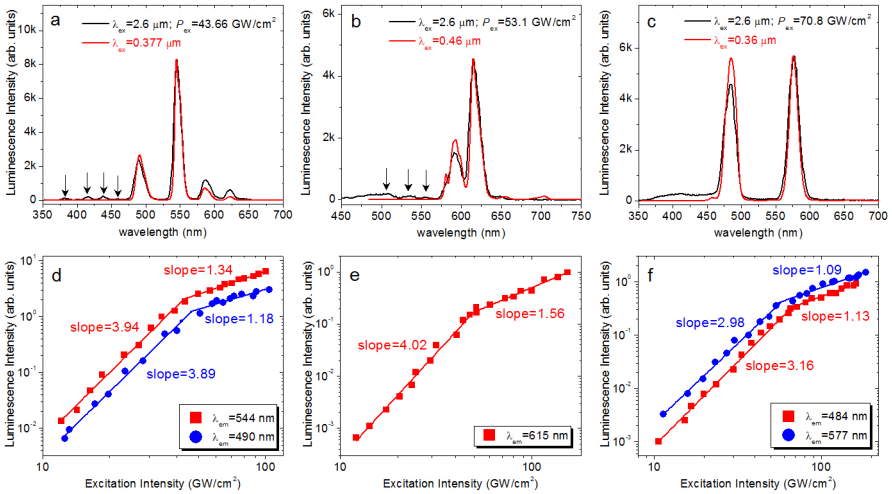


Fig. 3. Upconversion luminescence spectra (black curves) of the aluminoborate glasses doped with $Tb^{3+}$ (a), $Eu^{3+}$ (b), and $Dy^{3+}$ (c) under the excitation of 2.6-μm fs laser pulses. The corresponding downconversion luminescence spectra (red curves) for the three glasses are also provided for comparison. The new emission peaks observed in the $Tb^{3+}$- and $Eu^{3+}$-doped glasses are indicated by arrows. The dependence of the luminescence intensity on the excitation intensity for the three glasses are presented in (d), (e), and (f), respectively.

The emission spectra of the three glasses under the excitation of the 2.6-μm fs laser pulses are shown in Fig. 3. The photos showing the efficient upconversion luminescence under the excitation of the 2.6-μm fs laser pulses are presented in Fig. 4. At first glance, the spectra shapes appear to be quite similar to those observed under single photon excitation. However, a close inspection reveals the existence of some unique features resulting from the multiphoton excitation. As indicated by arrows in Fig. 3(a), one can see four new emissions peaking at 381, 416, 438, 460 nm in the $Tb^{3+}$-doped glass although their intensities are much weaker as compared with the major emission bands. They originate from the transitions of

#243906 Received 29 Jun 2015; revised 7 Aug 2015; accepted 9 Aug 2015; published 12 Aug 2015
© 2015 OSA

$^5D_3 \rightarrow {}^7F_6$, $^5D_3 \rightarrow {}^7F_5$, $^5D_3 \rightarrow {}^7F_4$, $^5D_3 \rightarrow {}^7F_3$ and the physical origin will be explained later. In the emission spectrum of the $Eu^{3+}$-doped glass shown in Fig. 3(b), one can identify three new emissions centered at 510, 540, and 555 nm, as indicated by the arrows. They are attributed to the transition of $^5D_2 \rightarrow {}^7F_3$, $^5D_2 \rightarrow {}^7F_4$, and $^5D_2 \rightarrow {}^7F_4$, respectively. For the $Dy^{3+}$-doped glass shown in Fig. 3(c), a broad emission band centered at ~410 nm is observed. In addition, the emission band centered at 483 nm becomes weaker than that centered at 575 nm. The intensities of these two emission bands are almost equal under the single photon excitation.

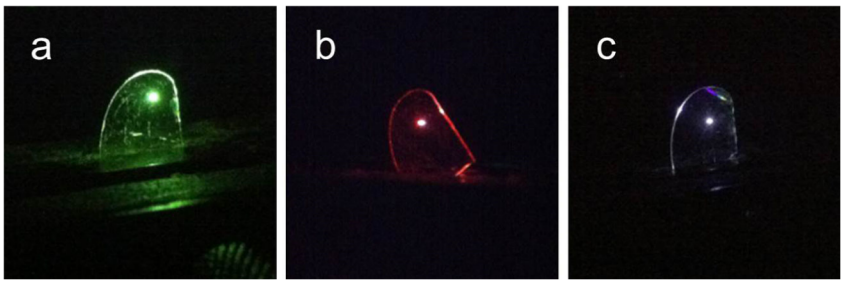


Fig. 4. Photos of the upconversion luminescence from the aluminoborate glasses doped with $Tb^{3+}$ (a), $Eu^{3+}$ (b), and $Dy^{3+}$ (c) under the excitation of 2.6-μm fs laser pulses with excitation power densities of 23.6, 35.4 and 53.1 GW/cm$^2$, respectively.

In order to gain a deep insight into the transition processes involved in the MPA processes in the glasses, we have examined the dependence of the luminescence intensity on the excitation intensity for the three glasses, as shown in Figs. 3(d)-3(f). For the $Tb^{3+}$- and $Eu^{3+}$-doped glasses, a slope of ~4.0 is observed in the low excitation intensity regime, implying a four-photon process is involved in the generation of the upconversion luminescence. For the $Dy^{3+}$-doped glass, the slope observed in the low excitation intensity regime is close to 3.0, indicating that the upconversion luminescence is induced mainly by a three-photon process. It has been confirmed that the dependence of the upconversion luminescence induced by the simultaneous absorption of n photons on the excitation power may exhibit a slope between n and 1, depending strongly on the pumping and decay rates for the intermediate states involved in the MPA process [27,28]. In the high excitation intensity regime, the slopes observed in the excitation power dependence of the luminescence intensity for all three samples are reduced to be ~1.1-1.5. For the cases in which the intermediate states are real states, it has been shown that the slope will eventually approach 1.0 at sufficiently high excitation intensities [27]. Similar change in the slope is also observed for various materials in which the intermediate states are virtual states and the simultaneous absorption of n photons is required [35–41]. Basically, this behavior is attributed to the saturation of the excited state involved in the multiphoton-induced absorption at high excitation intensities, such as the $^5D_4$ level for $Tb^{3+}$, the $^5D_0$ level for $Eu^{3+}$, and the $^4F_{9/2}$ level for $Dy^{3+}$ in our case.

For the generation of the upconversion luminescence, the wavenumber of the excitation light is 3846 cm$^{-1}$ while the largest wavenumber of the luminescence is 20833 cm$^{-1}$. It seems that the absorption of at least six photons is necessary for the generation of the upconversion luminescence. However, only a three- or four-photon process is involved according to the dependence of the luminescence intensity on the excitation intensity. It means that the intermediate states between the ground state and the high-energy state plays a crucial role in the MPA process, similar to what we have observed in the upconversion luminescence of $In_xGa_{1-x}N/GaN$ multiple quantum wells under the excitation of long-wavelength fs laser pulses [41].

In order to clearly understand the MPA-induced upconversion process, we examine the energy diagrams for the three rare-earth ions, as shown in Fig. 5. For the $Tb^{3+}$-doped glass, the largest energy gap appears between the $^7F_0$ and $^5D_4$ states, which is equal to the energy of four

#243906 Received 29 Jun 2015; revised 7 Aug 2015; accepted 9 Aug 2015; published 12 Aug 2015
© 2015 OSA

photons at 2.6 μm. It means that the population of the $^5D_4$ state can be achieved by simultaneously absorbing four photons at 2.6 μm provided that the $^7F_0$ state has been effectively populated through the super saturation phenomenon. As indicated by the arrows in Fig. 5(a), the effective population of the $^7F_0$ state can be realized by a consecutive transition $^7F_6 \xrightarrow{GSA} {}^7F_3 \xrightarrow{NR} {}^7F_5 \xrightarrow{ESA} {}^7F_0$. Here, GSA, ESA and NR represent ground state absorption, excited state absorption and nonradiative relaxation, respectively. It should be emphasized that the energy interval between the $^7F_0$ and $^7F_6$ states is equal to that between the $^5D_4$ and $^5D_3$ states. As a result, a cross relaxation in which the transition from the $^7F_0$ and $^7F_6$ states will initiate the transition from the $^5D_4$ and $^5D_3$ states may occur, as indicated in Fig. 5(a). It implies that the $^5D_3$ state can also be populated through the cross relaxation process. In general, the electrons on the $^5D_3$ state will relax nonradiatively to the $^5D_4$ state. In the case when the $^5D_3$ state is saturated, which is possible under the excitation of fs laser pulses, the radiative transitions from the $^5D_3$ state to the $^7F_{3,4,5,6}$ states will become possible, leading to the new emissions observed in the upconversion luminescence (see Fig. 3(a)).

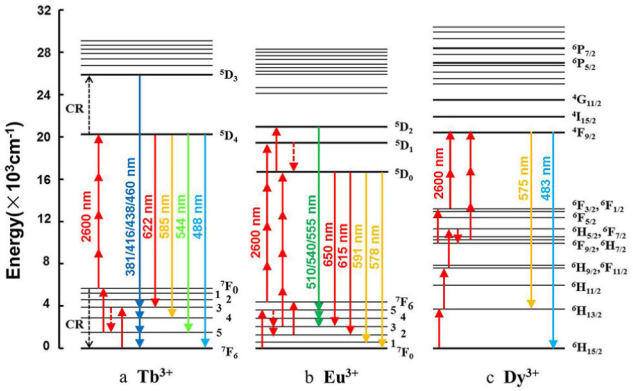


Fig. 5. Energy level diagrams for $Tb^{3+}$ (a), $Eu^{3+}$ (b), and $Dy^{3+}$ (c) ions in which the population of the high-energy levels induced by consecutive single-photon and multiphoton absorption and the generation of the upconversion luminescence are illustrated. CR denotes the cross relaxation process.

For the $Eu^{3+}$-doped glass, the largest energy gap appears between the $^7F_6$ and $^5D_0$ states and the absorption of four photons at 2.6 μm is required for the transition across the energy gap. There are two possible ways for realizing the effective population of the $^5D_0$ state, i.e. $^7F_0 \xrightarrow{GSA} {}^7F_5 \xrightarrow{NR} {}^7F_3 \xrightarrow{4ESA} {}^5D_0$ or $^7F_0 \xrightarrow{GSA} {}^7F_5 \xrightarrow{NR} {}^7F_2 \xrightarrow{ESA} {}^7F_6 \xrightarrow{4ESA} {}^5D_1 \xrightarrow{NR} {}^5D_0$, as indicated by arrows in Fig. 5(b). In both cases, a four-photon process is involved, in good agreement with the slope observed in the excitation-intensity-dependent luminescence (see Fig. 3(e)). Similarly, we can easily find out the two transition processes responsible for the upconverstion luminescence in the $Dy^{3+}$-doped glass. They can be describe as $^6H_{15/2} \xrightarrow{GSA} {}^6H_{13/2} \xrightarrow{ESA} {}^6H_{9/2} \xrightarrow{ESA} {}^6F_{7/2} \xrightarrow{NR} {}^6H_{7/2} \xrightarrow{3ESA} {}^4F_{9/2}$ or $^6H_{15/2} \xrightarrow{GSA} {}^6H_{13/2} \xrightarrow{ESA} {}^6H_{9/2} \xrightarrow{ESA} {}^6F_{7/2} \xrightarrow{NR} {}^6F_{9/2} \xrightarrow{ESA} {}^6F_{1/2} \xrightarrow{2ESA} {}^4F_{9/2}$, as indicated in Fig. 5(c). Apparently, a three-photon process is needed to generate the upconversion luminescence, in accordance with the slope observed in Fig. 3(f).

*3.3 Upconversion luminescence under multiphoton excitation in thick glass samples*

The upconversion luminescence described above was observed in thin glass samples with a thickness of 0.5 mm, as shown in Fig. 4. No obvious change in the spectral shape was observed with increasing excitation intensity. In thick glass samples, however, the discrete

#243906 Received 29 Jun 2015; revised 7 Aug 2015; accepted 9 Aug 2015; published 12 Aug 2015
© 2015 OSA

emission bands in the luminescence spectrum are significantly broadened at high excitation intensities, leading to the change of the luminescence color, as shown in Fig. 6. Although the spectra have evolved from discrete emission bands to continuous emission bands, the original emission peaks can still be identified in the spectra. We think that the broadening of the emission bands in the thick glass samples is caused by the self-focusing of the laser beam which leads to a dramatic increase in the excitation intensity. A close inspection reveals the formation of filamentation inside the glass samples, verifying the self-focusing effect [42]. Owing to the significantly enhanced excitation intensity, various high-order nonlinear optical processes become efficient, leading to the generation of new frequency components. Basically, the number of photons required for the generation of these broadband emissions is the same as that for the generation of upconversion luminescence in the thin glass samples which we have discussed above. Actually, similar broadening of emission bands has been observed by different groups in different materials. For example, Liu et al. discovered the novel ciliary white light generation around the fundamental frequency in transparent materials (including glasses, crystals, and polymers) excited by 800-nm fs laser pulses [43]. The supercontinuum generation near the third-harmonic region in a YAG crystal has been studied by Silva et al. [44]. Furthermore, Durand et al. experimentally investigated the extreme blueshifted broad supercontinuum generation in the visible region from fused silica under the excitation of near-infrared fs pulses ranging from 1.2 to 2.4 μm [45]. These phenomena are quite similar to the broadened luminescence around the discrete emission bands observed in this work.

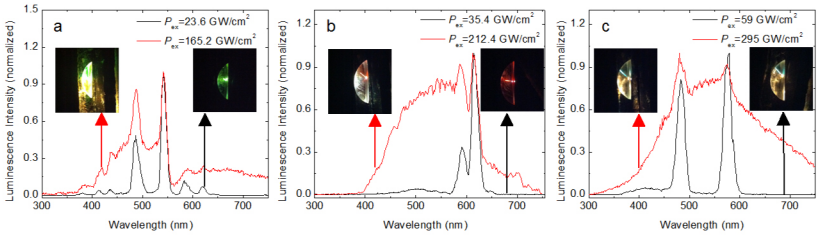


Fig. 6. Normalized emission spectra of the thick aluminoborate glasses doped with $Tb^{3+}$ (a), $Eu^{3+}$ (b), and $Dy^{3+}$ (c) under the excitation of 2.6-μm fs laser pulses with low (black curves) and high (red curves) excitation intensities. The photos of the upconversion luminescence from the aluminoborate glasses are shown in the insets.

Owing to the potential applications of rare-earth-ion-doped nanoparticles in bioimaging, we are trying to study the upconversion luminescence of rare-earth-ion-doped glasses under the excitation of long-wavelength fs laser pulses. So far, most previous works in this field focus mainly on the cooperative multiphoton luminescence in which two or more rare-earth ions are generally involved. In this case, the laser excitation is initially absorbed by a sensitizer ion and subsequently transferred to an acceptor ion that is responsible for the upconversion luminescence [29–32,34]. In addition, the longest excitation wavelength used for generating the upconversion luminescence is about 1.5 μm. In this work, we demonstrate that the efficient upconversion luminescence can also be achieved in the glasses doped with only one type of ion under the excitation wavelength as long as 2.6 μm. It is clarified that the simultaneous absorption of only three or four photons are involved in the generation of the upconversion luminescence because of the existence of many intermediate states in the rare-earth ions. By exploiting the super saturation phenomenon, the excitation power density necessary for the generation of the upconversion luminescence is reduced significantly. A significantly broadened emission bands can be achieved by utilizing the self-focusing effect occurring in the thick glass samples. Finally, the large anti-stock shift (i.e., the separation between the upconversion luminescence and the excitation light) will be helpful for improving the signal-to-noise ratio in bioimaging [46].

#243906 Received 29 Jun 2015; revised 7 Aug 2015; accepted 9 Aug 2015; published 12 Aug 2015
© 2015 OSA

## 4. Conclusion

In summary, we have investigated the upconversion luminescence generated in three aluminoborate glasses doped with $Tb^{3+}$, $Eu^{3+}$, and $Dy^{3+}$ by using 2.6-μm fs laser pulses. Efficient upconversion luminescence was achieved by exploiting the super saturation phenomenon. It was identified that a four-photon process is involved in the generation of the upconversion luminescence in the $Tb^{3+}$- and $Eu^{3+}$-doped glasses while a mixed two- and three-photon process is involved in the $Dy^{3+}$-doped glass. In thick glass samples, the luminescence was found to be significantly broadened due to the self-focusing of the laser beam, leading to the change in the upconversion luminescence. The efficient upconversion luminescence generated by long-wavelength fs laser pulses will find potential applications in the fields of color display and bioimaging.

## Acknowledgments

The authors acknowledge the financial support from the National Natural Science Foundation of China (Grant Nos. 51171066, 11374109, and 11204092).

#243906 Received 29 Jun 2015; revised 7 Aug 2015; accepted 9 Aug 2015; published 12 Aug 2015
© 2015 OSA